Carcinogenesis, 2018, Vol. 39, No. 2, 134–145

doi:10.1093/carcin/bgx114
Advance Access publication October 11, 2017
Original Article

ORIGINAL ARTICLE

Prevention of breast cancer-induced osteolytic bone resorption by benzyl isothiocyanate

Subrata K. Pore[1], Eun-Ryeong Hahm[1], Joseph D. Latoche[2,3], Carolyn J. Anderson[2,3], Yongli Shuai[4] and Shivendra V. Singh[1,2,*]

[1]Department of Pharmacology and Chemical Biology, University of Pittsburgh School of Medicine, Pittsburgh, PA, USA; [2]Department of Medicine, University of Pittsburgh School of Medicine, Pittsburgh, PA, USA; [3]*In Vivo* Imaging Facility, UPMC Hillman Cancer Center, University of Pittsburgh School of Medicine, Pittsburgh, PA, USA; [4]Biostatistics Facility, UPMC Hillman Cancer Center, University of Pittsburgh School of Medicine, Pittsburgh, PA, USA

*To whom correspondence should be addressed. Tel: +1 412 623 3263; Fax: +1 412 623 7828; E-mail: singhs@upmc.edu

Abstract

Osteolytic bone resorption is the primary cause of pain and suffering (e.g. pathological bone fracture) in women with metastatic breast cancer. The current standard of care for patients with bone metastasis for reducing the incidence of skeletal complications includes bisphosphonates and a humanized antibody (denosumab). However, a subset of patients on these therapies still develops new bone metastasis or experiences adverse effects. Moreover, some bisphosphonates have poor oral bioavailability. Therefore, orally-bioavailable and non-toxic inhibitors of breast cancer-induced osteolytic bone resorption are still clinically desirable. We have shown previously that benzyl isothiocyanate (BITC) decreases the incidence of breast cancer in a transgenic mouse model without any side effects. The present study provides *in vivo* evidence for inhibition of breast cancer-induced osteolytic bone resorption by BITC. Plasma achievable doses of BITC (0.5 and 1 μM) inhibited *in vitro* osteoclast differentiation induced by co-culture of osteoclast precursor cells (RAW264.7) and breast cancer cells representative of different subtypes. This effect was accompanied by downregulation of key mediators of osteoclast differentiation, including receptor activator of nuclear factor-κB ligand and runt-related transcription factor 2 (RUNX2), in BITC-treated breast cancer cells. Doxycycline-inducible knockdown of RUNX2 augmented BITC-mediated inhibition of osteoclast differentiation. Oral administration of 10 mg BITC/kg body weight, 5 times per week, inhibited MDA-MB-231-induced skeletal metastasis multiplicity by ~81% when compared with control ($P = 0.04$). The present study indicates that BITC has the ability to inhibit breast cancer-induced osteolytic bone resorption *in vivo*.

Introduction

Despite significant progress in our knowledge concerning the risk factors and genomic heterogeneity of breast cancer, this malignancy remains a leading cause of cancer-linked deaths in women worldwide (1–5). Metastatic spread to distant organs is the primary cause of morbidity and mortality in patients with breast cancer (6–10). Women with breast cancer may experience metastasis to the bone, lung, liver, and brain, but skeleton is the preferred site of metastatic spread for each subtype of the disease (ranges between 43 and 71%) when compared with other sites (8–47%) (11). Incidence of skeletal metastasis varies from up to 71% for luminal-type to 60% for human epidermal growth factor receptor 2+ to 39–43% for basal-like breast cancers (11). The homeostatic balance between new bone formation resulting from activation of osteoblasts (mono-nucleated cells of mesenchymal stem cell lineage) and osteolytic bone resorption triggered by activation of osteoclasts (multi-nucleated cells of hematopoietic lineage) is severely compromised in skeletal metastasis (8–10). Majority of the bone lesions associated with human breast cancers are osteolytic (6–10). Secondary tumors within the bone are responsible for major complications in patients with breast cancer, including pathological fractures, disability, nerve compression syndrome, pain and hypercalcemia

Received: June 29, 2017; **Revised:** September 26, 2017; **Accepted:** October 6, 2017

Abbreviations

BITC	benzyl isothiocyanate
BSA	bovine serum albumin
CM	conditioned medium
CT	computed tomography
DMSO	dimethyl sulfoxide
FBS	fetal bovine serum
GAPDH	glyceraldehyde-3-phosphate dehydrogenase
M-CSF	macrophage colony-stimulating factor
PBS	phosphate-buffered saline
OPG	osteoprotegerin
RANKL	receptor activator of nuclear factor-κB ligand
RUNX2	runt-related transcription factor 2
sRANKL	soluble RANKL
T47D/sh-RUNX2^{Dox}	doxycycline-inducible stable RUNX2 knockdown T47D cells
TCGA	The Cancer Genome Atlas
TRAP	tartrate-resistant acid phosphatase

(6,7,9,10). Identification of safe and inexpensive agents with the ability to inhibit the development of osteolytic bone lesions is clinically attractive because the currently available options are suboptimal (12,13).

Phytochemicals in edible and medicinal plants continue to attract research interest for identification of promising cancer preventative agents (14–17). Intrigued by the results of epidemiological studies suggesting an inverse association between dietary-intake of cruciferous vegetables and the risk of breast cancer, we and others have investigated the cancer chemopreventative potential of phytochemicals unique to this plant family, including isothiocyanates and indoles (18–21). Benzyl isothiocyanate (BITC) is one such phytochemical whose cancer chemopreventative potential has been studied using preclinical rodent models (22,23). The breast cancer in Sprague–Dawley rats induced by the environmental carcinogen 7,12-dimethylbenz[*a*] anthracene was inhibited significantly by BITC administration in a pre-initiation setting (22). We were the first to study post-initiation breast cancer chemoprevention by BITC in a transgenic mouse model (23). Dietary administration of BITC (3 μmol/g diet) for 25 weeks decreased the incidence and/or burden of mammary hyperplasia and carcinoma without weight loss or any other side-effects (23). BITC-mediated prevention of mammary carcinogenesis in this mouse model was associated with suppression of cell proliferation, increased apoptosis, and induction of E-cadherin protein expression (23).

Loss of E-cadherin expression with a concomitant increase in mesenchymal marker protein levels (e.g. vimentin) is a biochemical hallmark of epithelial-to-mesenchymal transition, a normal physiological process that is also implicated in cancer metastasis (24,25). Because BITC inhibits epithelial-to-mesenchymal transition (26), it was of interest to determine its effect on breast cancer-induced osteoclast differentiation and osteolytic bone resorption using *in vitro* and *in vivo* models.

Materials and methods

Ethics statement

Use of mice for the experiment described herein was approved by the Institutional Animal Care and Use Committee of the University of Pittsburgh.

Reagents

BITC (purity >98%) was purchased from LKT laboratories (St. Paul, MN). Stock solution of BITC (500 μM) was prepared in dimethyl sulfoxide (DMSO) and diluted with medium (final concentration of DMSO was 0.4%). Reagents for cell culture, including fetal bovine serum (FBS), culture media, and antibiotic mixture, were purchased from Life Technologies-Thermo Fisher Scientific (Waltham, MA). Antibodies against receptor activator of nuclear factor-κB ligand (RANKL, 1:200 dilution), nuclear factor-κB, p65 subunit (1:1000 dilution) and runt-related transcription factor 2 (RUNX2) for immunofluorescence (1:50 dilution) were purchased from Santa Cruz Biotechnology (Dallas, TX). An antibody against RUNX2 for western blotting (1:250 dilution) was purchased from MBL international (Woburn, MA). Antibodies against osteoprotegerin (OPG; 1:500 dilution) and glyceraldehyde-3-phosphate dehydrogenase (GAPDH, 1:50 000 dilution) were purchased from GeneTex (Irvine, CA). Recombinant murine soluble RANKL (sRANKL) and murine macrophage colony-stimulating factor (M-CSF) were purchased from PeproTeck (Rocky Hill, NJ). A kit for determination of sRANKL was purchased from Enzo Life Sciences (Farmingdale, NJ). RANKL levels in mice plasma were measured using a kit from Abcam (Cambridge, MA). Cathepsin K activity was determined using a fluorometric kit from BioVision (Milpitas, CA). A kit for determination of interleukin-8 (IL-8) levels in mouse plasma was purchased from MyBioSource (San Diego, CA).

Cell lines

Osteoclast precursor RAW264.7 cells and breast cancer cell lines (MDA-MB-231, SK-BR-3 and MCF-7) were purchased from American Type Culture Collection (Manassas, VA). Cultures of MDA-MB-231, MCF-7 and SK-BR-3 cell lines were last authenticated in March 2017. RAW264.7 cells were cultured in Dulbecco's modified essential medium supplemented with 10% FBS and antibiotic mixture containing penicillin, streptomycin and neomycin. Monolayer cultures of MDA-MB-231, MCF-7 and SK-BR-3 cells were maintained as recommended by the supplier. Each cell line was maintained at 37°C in 5% CO_2 in a humidified incubator. Doxycycline (Dox)-inducible stable RUNX2 knockdown T47D cells (T47D/sh-RUNX2^{Dox}) were generously provided by Dr. Baruch Frenkel (University of Southern California, CA). T47D/sh-RUNX2^{Dox} cells were cultured in RPMI 1640 medium supplemented with 10% FBS. About 250 ng/ml Dox in water (Sigma-Aldrich, St. Louis, Los Angeles, MO) was used to initiate knockdown of RUNX2.

Trypan blue dye exclusion assay

Osteoclast precursor RAW264.7 cells were plated in triplicate in 12-well plates at a density of 25 000 cells per well. Cells were treated with DMSO or different concentrations of BITC for 72 h, washed with phosphate-buffered saline (PBS), and stained with 0.1% trypan blue solution. Live cells were counted under an inverted microscope.

Osteoclast differentiation assay

Effect of BITC treatment on osteoclast differentiation was assessed by tartrate-resistant acid phosphatase (TRAP) staining with three different protocols for stimulation of osteoclast differentiation, including (i) co-culture of RAW264.7 cells with breast cancer cells, (ii) addition of conditioned media (CM) from breast cancer cells to RAW264.7 cells and (iii) addition of sRANKL and M-CSF to RAW264.7 cells. For the co-culture experiment, RAW264.7 cells were plated in 24-well plates in triplicate at a density of 2500 cells per well and kept overnight to adhere. Next day, breast cancer cells (MDA-MB-231, MCF-7 or SK-BR-3) were added to RAW264.7 cells at a ratio of 2.5:1 and treated with DMSO (control) or different concentrations of BITC. The cell monolayer was gently washed with PBS and fixed with a solution containing 37% formaldehyde, acetone and citrate. TRAP assay was done using a kit from Sigma-Aldrich according to manufacturer's protocol. Cells were stained with hematoxylin solution to stain nuclei. The osteoclasts were counted manually and photographed under a Leica DMIRB microscope equipped with DFC450C digital camera at ×200 magnification. In a separate experiment, T47D/sh-RUNX2^{Dox} cells were either untreated or treated with 250 ng/ml Dox for 24 h and then added to RAW264.7 cells at a ratio of 2.5:1. The TRAP-positive osteoclasts were scored after 6 days.

For the second protocol involving stimulation of osteoclast differentiation by CM, MDA-MB-231 and SK-BR-3 cells were plated in 100-mm culture dishes. After reaching 70–80% confluency, the cells were maintained in serum-free RPMI 1640 medium overnight. Cells were then treated

with DMSO or different concentrations of BITC in serum-free RPMI1640 medium. After 48 h of treatment, CM was collected and centrifuged to remove cell debris and stored at -20°C. RAW264.7 cells were plated in 24-well plates at a density of 2500 cells per well, kept overnight to adhere and then 50% CM was added to RAW264.7 cells. TRAP staining was performed 6 days after addition of CM as described previously.

For the third protocol, RAW264.7 cells were plated in 24-well plates at a density of 2500 cells per well and kept overnight to adhere. The medium was replaced with fresh medium supplemented with 100 ng/ml murine sRANKL and 30 ng/ml murine M-CSF, DMSO or different concentrations of BITC. After 6 days, TRAP staining was done as described previously.

Determination of sRANKL level

Levels of sRANKL in cell lysates and CM of control (DMSO-treated) and BITC-treated breast cancer cells or CM of co-cultures of RAW264.7 cells and breast cancer cells were determined using a commercially available kit and following the manufacturer's protocol.

Western blotting

Whole cell lysates from cells and tumor supernatants from control- and BITC-treated MMTV-*neu* mice were prepared as described by us previously (27–29). Western blotting was done as described previously (27,28). Immunoreactive bands were quantified by densitometric analysis using UN-SCAN-IT software version 5.1 (Silk Scientific, Orem, UT).

Confocal microscopy

Desired cells (25 000 cells per well) were plated in 24-well plates in triplicate on coverslips and allowed to adhere by overnight incubation. Cells were treated with DMSO or different concentrations of BITC for 24 h. Cells were fixed with 2% paraformaldehyde overnight at 4°C, permeabilized with 0.5% Triton X-100 for 10 min, and then blocked with 0.5% bovine serum albumin (BSA) and 0.15% glycine in PBS for 1 h at room temperature. This was followed by incubation with RUNX2 antibody (1:50 dilution) overnight at 4°C. The cells were washed and incubated with Alexa Fluor 488-conjugated secondary antibody (1:2000 dilution, Life Technologies) for 1 h at room temperature. Nuclei were stained with DRAQ5 (1:10 000 dilution) for 10 min at room temperature. Stained cells were observed under a Leica confocal TCSSL microscope at ×63 objective magnification in oil.

Real-time quantitative polymerase chain reaction

Cells were treated with DMSO or different concentrations of BITC for 24 h. Total RNA was isolated using a kit from Qiagen (Germantown, MD). The complementary DNA was synthesized from 1 µg of RNA with the use of SuperScript III reverse transcriptase and oligo$(dT)_{20}$ primer. Polymerase chain reaction was performed using SYBR green master mix at 95°C (15 s), 60°C (60 s) for annealing and 72°C (30 s) for 40 cycles. GAPDH was used as a control. Primers were as follows: *IL-1β* Forward: 5′-ATGGCAGAAGTACCTAAGCTCGC-3′; *IL-1β* Reverse: 5′-ACACAAATTGCATGGTGAAGTCAGTT-3′; *IL-6* Forward: 5′-GGTACATCCTCGACGGCATCT-3′; *IL-6* Reverse: 5′-GTGCCTCTTTGCTGCTTTCAC-3′; *IL-8* Forward: 5′-ATGACTTCCAAGCTGGCCGT-3′; *IL-8* Reverse: 5′-CCTCTTCAAAAACTTCTCCACACC-3′; *IL-11* Forward: 5′-TCTCTCCTGGCGGACACG-3′; *IL-11* Reverse: 5′-AATCCAGGTTGTGGTCCCC-3′; *TNF-α* Forward: 5′-GCCATTGGCCAGGAGGGC-3′, *TNF-α* Reverse: 5′-CGCCACCACGCTCTTCTG-3′; *MMP-9* Forward: 5′-TTGACAGCGACAAGAAGTGG-3′, *MMP-9* Reverse: 5′-GCCATTCACGTCGTCCTTAT-3′; *MMP-13* Forward: 5′-TCCCAGGAATTGGTGATAAAGTAGA-3′, *MMP-13* Reverse: 5′-CTGGCATGACGCGAACAATA-3′; *RUNX2* Forward: 5′-GCTGTTATGAAAAACCAAGT-3′; *RUNX2* Reverse: 5′-GGGAGGATTTGTGAAGAC-3′; *GAPDH* Forward: 5′-GGACCTGACCTGCCGTCTGAA-3′; *GAPDH* Reverse: 5′-GGTGTCGCTGTTGAAGTCGAG-3′. Relative gene expression was calculated using the method of Livak *et al.* (30).

Determination of cathepsin K activity

Cathepsin K activity was determined in: (i) CM collected after 6 days of co-culture of RAW264.7 and MDA-MB-231 cells in the absence (DMSO) or presence of BITC (0.5 or 1 µM), and (ii) CM from RAW264.7 collected after 6 days of treatment with sRANKL (100 ng/ml) plus M-CSF (30 ng/ml). Cathepsin K activity was determined using a fluorometric kit and by following the manufacturer's protocol. The fluorescence was measured at 400 nm excitation and 500 nm emission wavelengths.

In vivo study

Power calculation was based on a previously published study (31). It was estimated that a sample size of 10 mice per group would be required to achieve at least 80% power to detect a 50% mean difference in skeletal metastasis incidence at a significance level of 0.05 assuming a coefficient of variation of 0.3. Eighteen BALB/C-nu/nu female mice of ~4 weeks of age were purchased from Charles River Laboratories (Wilmington, MA). Luciferase-expressing MDA-MB-231 cells were cultured in minimum essential medium supplemented with 10% FBS, non-essential amino acids, L-glutamine, sodium pyruvate and antibiotic mixture at 37°C. After reaching 80–90% confluency, cells were trypsinized, washed and re-suspended in ice-cold PBS at a cell density of 10^6 cells per ml. At ~5 weeks of age, mice were anesthetized with 2.5% isoflurane and its concentration was maintained during the procedure. Cell suspension (100 µL) was injected into the left ventricle of each mouse using 27.5G needle. Mice were randomized into two groups: (i) control group (n = 9) and (ii) BITC treatment group (n = 9). One day after tumor cell injection, experimental group of mice received 10 mg BITC/kg body weight in corn oil by oral intubation 5 times per week (Monday to Friday). The control group of mice received corn oil only by oral intubation 5 times per week (Monday-Friday). One mouse from the BITC treatment group died one week prior to the sacrifice due to complications from anesthesia during bioluminescence imaging. However, bone metastasis data were available for this mouse and hence included in the final analysis. Body weights of the mice were recorded weekly. Bioluminescence imaging was done once a week using IVIS200 with FOV 25.8 and binning 8 (Xenogen-PerkinElmer, Waltham, MA). Ten minutes prior to imaging, 150 µL D-luciferin solution was injected via intraperitoneal route from a 100 mM stock. Maximum exposure time to get bioluminescence image was 5 min.

Small animal computed tomography (CT)

CT imaging was performed on the Siemens Inveon Multi-modality positron emission tomography/CT scanner. Scans were done at low/medium magnification (220 projections, 60kV/500 µA with a 950 ms exposure) with a 50 mm axial field of view at 2 × 2 binning. CT reconstructions were done using Siemens' Feldkamp algorithm with low noise reduction and Shepp-Logan filtering at a downsampling = 0. Images were viewed and analyzed in Siemens Inveon Research Workplace software. At the end of animal study, mice were euthanized by CO_2 inhalation and bones were collected. Bones were fixed in 10% neutral-buffered formalin for 48 h and decalcified using a decalcification solution for 24 h. Samples were transferred in 70% ethanol and embedded in paraffin for sectioning. Bone sections were stained with hematoxylin and eosin and imaged under microscope at ×200 magnification.

Cytokine profiling

Blood was collected from mice at the time of sacrifice in heparin-coated syringes. Blood samples were centrifuged at 1000 *g* for 10 min at 4°C. Supernatants were collected and stored at –20°C. Fluorokine_MAP cytokine multiplex kit was used for the Luminex assay.

Determination of IL-8 level in mouse plasma

IL-8 levels in mice plasma were determined using a kit from MyBioSource (San Diego, CA) and by following manufacturer's protocol.

Analysis of RNA-seq expression profile in The Cancer Genome Atlas (TCGA)

RUNX2 and *RANKL (TNFSF11)* RNA-seq expression profiles in different subtypes of human breast cancer in the TCGA dataset were determined using University of California Santa Cruz Xena Browser (http://xena.ucsc.edu/public-hubs/). *RUNX2* and *RANKL* expressions were compared among different subtypes of breast cancer and normal breast tissues.

Statistical tests

Statistical significance of differences for dose–response comparisons were determined by one-way analysis of variance with Dunnett's adjustment. One-way analysis of variance followed by Bonferroni's test was used for multiple comparisons, including comparison of RNA-seq expression profiles for *RUNX2* and *RANKL*. For two sample comparisons, unpaired Student's *t*-test was used. Fisher's exact test was used for analysis of bone metastases incidence. A significance level was set at 0.05. Statistical analyses were performed using a GraphPad Prism (v 7.02, GraphPad Software, La Jolla, CA). All statistical tests were two-sided.

Results

Effect of BITC on osteoclast differentiation

Breast cancer-associated skeletal metastases are predominantly osteolytic (bone destructing) caused by activation of osteoclasts, which are derived from hematopoietic stem cells (6–10). Initially, we performed trypan blue dye exclusion assay to find out BITC (structure is shown in Figure 1A) concentrations that were within the plasma achievable range (32) but non-cytotoxic to RAW264.7. BITC concentrations up to 1 μM were non-toxic to RAW264.7 cells (data not shown). Because skeletal metastasis is prevalent in all major subtypes of breast cancer (11), well-characterized representative of basal-like (MDA-MB-231), luminal-type (MCF-7) and estrogen receptor-negative, but human epidermal growth factor receptor 2 amplified (SK-BR-3), breast cancer cells (33) were used for osteoclast differentiation assay. The number of TRAP-positive osteoclasts, which were not observed in RAW264.7 cultures (Figure 1B; identified by a circle), was increased upon co-culture of RAW264.7 with each breast cancer cell line as shown for MDA-MB-231 cells in Figure 1C. The numbers of breast cancer-induced osteoclasts were decreased dose-dependently in the presence of BITC for each cell line (Figure 1C).

In a separate but complimentary experiment, osteoclast differentiation was assessed 6 days after addition of CM collected from MDA-MB-231 or SK-BR-3 cells to RAW264.7. Osteoclast differentiation in RAW264.7 cells was stimulated by addition of CM from DMSO-treated breast cancer cells (Figure 1D), which was decreased when CM from BITC-treated cells was added to RAW264.7 cells (Figure 1D,E). Osteoclast differentiation in RAW264.7 cells stimulated by exposure to sRANKL + M-CSF cocktail was also inhibited in the presence of BITC (Figure 1F). These results demonstrated BITC-mediated inhibition of osteoclast differentiation in RAW264.7 cells *in vitro*.

Effect of BITC on sRANKL expression and secretion

The tumor necrosis factor super-family member RANK receptor, its ligand (RANKL) and a naturally occurring decoy receptor of RANKL (OPG) play an important role in bone remodeling and in skeletal metastasis (34,35). Expression of RANKL, which is either membrane-associated or soluble, has been observed in breast cancer cells (34–36). Exposure of MDA-MB-231 cells to BITC resulted in a dose-dependent decrease in expression (Figure 2A) and secretion of sRANKL (Figure 2B), especially at the 48-h time point. BITC-mediated decrease in sRANKL secretion was also evident in CM collected after 6 days of co-culture of RAW264.7 and MDA-MB-231 cells (Figure 2C). Western blotting confirmed BITC-mediated decrease in sRANKL protein expression in MDA-MB-231, MCF-7 and SK-BR-3 cell lines (Figure 2D). A transient increase in protein level of OPG was also observed at 24-h time point (Figure 2D), leading to a decrease in the ratio of sRANKL/OPG in each cell line (Figure 2E). These results indicated that inhibition of breast cancer-induced osteoclast differentiation in the presence of BITC was accompanied by suppression of sRANKL expression and secretion.

Role of RUNX2 in BITC-mediated inhibition of osteoclast differentiation

We next studied the effect of BITC treatment on expression of RUNX2, which is a transcription factor implicated in regulation of RANKL expression and skeletal metastasis and in breast carcinogenesis (37–39). Confocal microscopy revealed nuclear localization of RUNX2 protein in DMSO-treated cells (Figure 3A). Nuclear level of RUNX2 was markedly decreased after 24 h of treatment with BITC in each cell line (Figure 3A). BITC treatment also resulted in a decrease in mRNA levels of *RUNX2* in each cell line (Figure 3B).

We used T47D breast cancer cells with Dox-inducible knockdown of RUNX2 (T47D/shRUNX2^{Dox}) to further study its role in BITC-mediated inhibition of osteoclast differentiation. RUNX2 protein level was decreased by ~70% 24 h after addition of Dox, and this effect was augmented upon BITC treatment (Figure 3C). A similar pattern was seen for sRANKL protein expression (Figure 3C). As expected, Dox-induced knockdown of RUNX2 alone inhibited osteoclast differentiation by ~28%, which was augmented in the presence of BITC (Figure 3D).

Effect of BITC on osteoclast differentiation regulating factors

Skeletal metastasis is a complex process involving tumor cell invasion to the bone followed by recruitment of osteoclast precursors, osteolytic bone resorption leading to release of growth factors from bone matrix that can fuel tumor growth (10,40,41). Molecules produced by tumor cells (e.g. IL-8 and IL-11) can also stimulate osteoclast activity. We therefore determined the effect of BITC treatment on mRNA expression of osteoclast regulating molecules using MDA-MB-231 and SK-BR-3 cells (Figure 4A). BITC-treated cells exhibited a decrease in mRNA levels of *IL-1β*, *IL-11*, *IL-6*, *TNF-α*, *IL-8*, *MMP-9*, and *MMP-13* especially at the 1 μM concentration (Figure 4A).

Effect of BITC on cathepsin K activity

Cathepsin K is a cysteine protease that is expressed in osteoclasts and plays an important role in degradation of the demineralized collagen matrix (42). Cathepsin K is also overexpressed in breast cancer cells metastasizing to the bone (43). Cathepsin K activity was modestly but significantly higher in the CM of RAW264.7 + MDA-MB-231 co-cultures compared with CM of RAW264.7 cells alone (Figure 4B). Cathepsin K activity in CM of RAW264.7 + MDA-MB-231 co-cultures was decreased in the presence of BITC (Figure 4B). Similar results were observed in experiments where CM from RAW264.7 cells was collected after 6 days of stimulation with sRANKL + M-CSF cocktail (Figure 4C).

Effect of BITC on MDA-MB-231-induced skeletal metastasis *in vivo*

The effect of oral BITC administration on skeletal metastasis induced by intra-cardiac injection of luciferase-expressing MDA-MB-231 cells was assessed by longitudinal bioluminescence imaging and small animal CT. Representative bioluminescence and CT images of mice of the control and BITC treatment groups prior to sacrifice are shown in Figure 5A (metastasis site is identified by an arrow and the red circle shows site of bone resorption in mouse # B21L). Figure 5B shows longitudinal bioluminescence and CT imaging for one mouse each of the control and BITC treatment groups. The overall incidence of bone

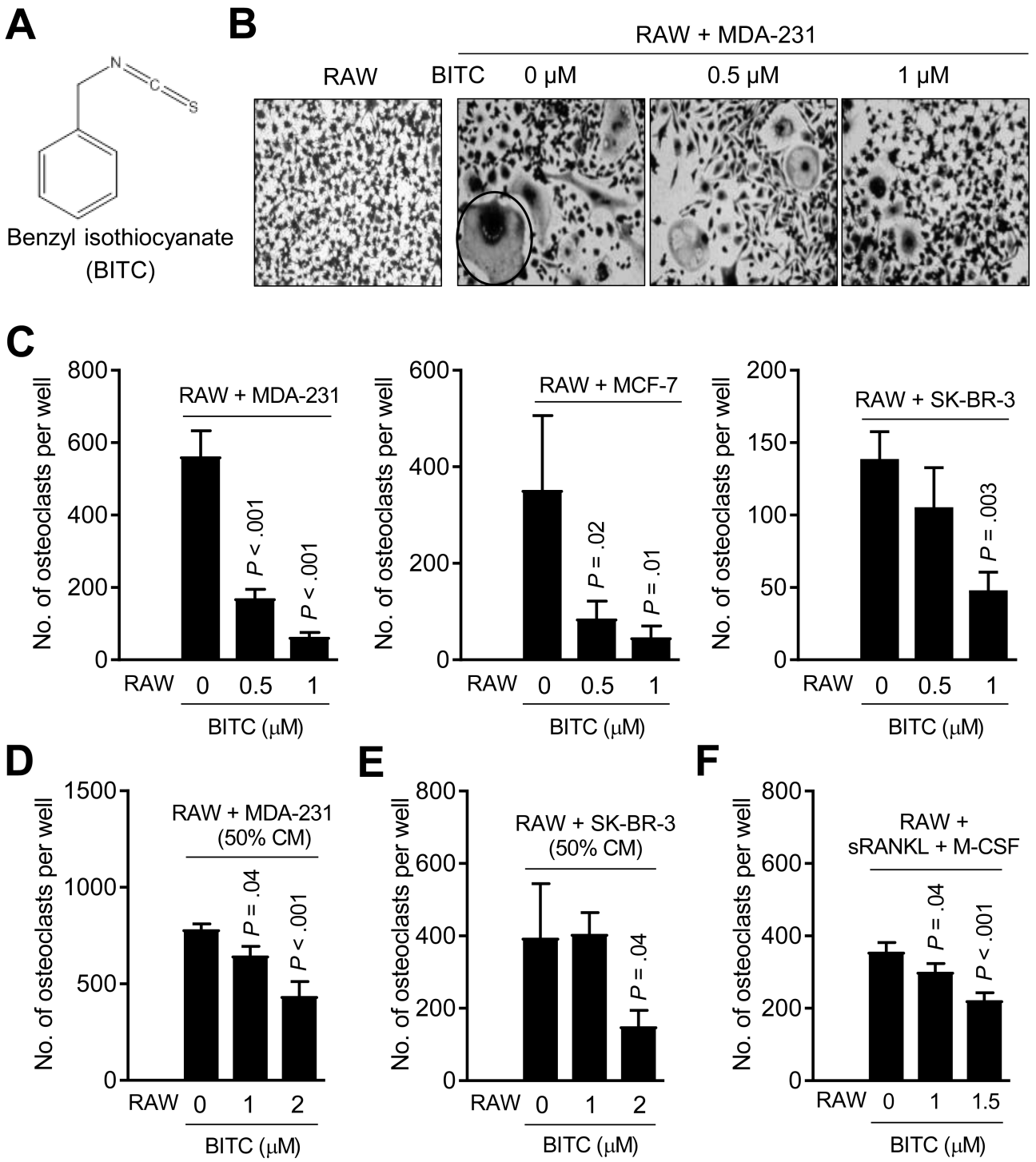

Figure 1. BITC treatment inhibits human breast cancer-induced osteoclast differentiation *in vitro*. (**A**) Chemical structure of BITC. (**B**) Representative microscopic images (×200 magnification) depicting osteoclasts (circled) in co-cultures of RAW264.7 (RAW) and MDA-MB-231 (MDA-231) cells after treatment with DMSO or the indicated doses of BITC for 6 days. Osteoclast differentiation was not observed in RAW264.7 cells alone. (**C**) Quantitation of osteoclast number in co-cultures of RAW264.7 (RAW) and specified breast cancer cells after treatment with DMSO or the indicated doses of BITC for 6 days. Quantitation of osteoclast number in RAW264.7 (RAW) cultured for 6 days with CM from MDA-MB-231 (MDA-231) (**D**) or SK-BR-3 cells (**E**) with or without BITC treatment. (**F**) Effect of BITC treatment on osteoclast number in RAW264.7 (RAW) stimulated by addition of sRANKL (100 ng/ml) and M-CSF (30 ng/ml) for 6 days. Columns indicate average of triplicate samples from a representative experiment, and bars indicate standard deviation. *P* value was determined by one-way analysis of variance with Dunnett's adjustment. Consistent results were obtained in at least two independent experiments.

metastasis in the BITC treatment group was lower by ~67% when compared with control (Figure 5C). Nevertheless, several mice of the BITC treatment group exhibited complete regression of bone metastasis based on bioluminescence signal. For example, bioluminescence in the hind limb or spine of mouse # B31R was visible until week 5, but this signal disappeared thereafter.

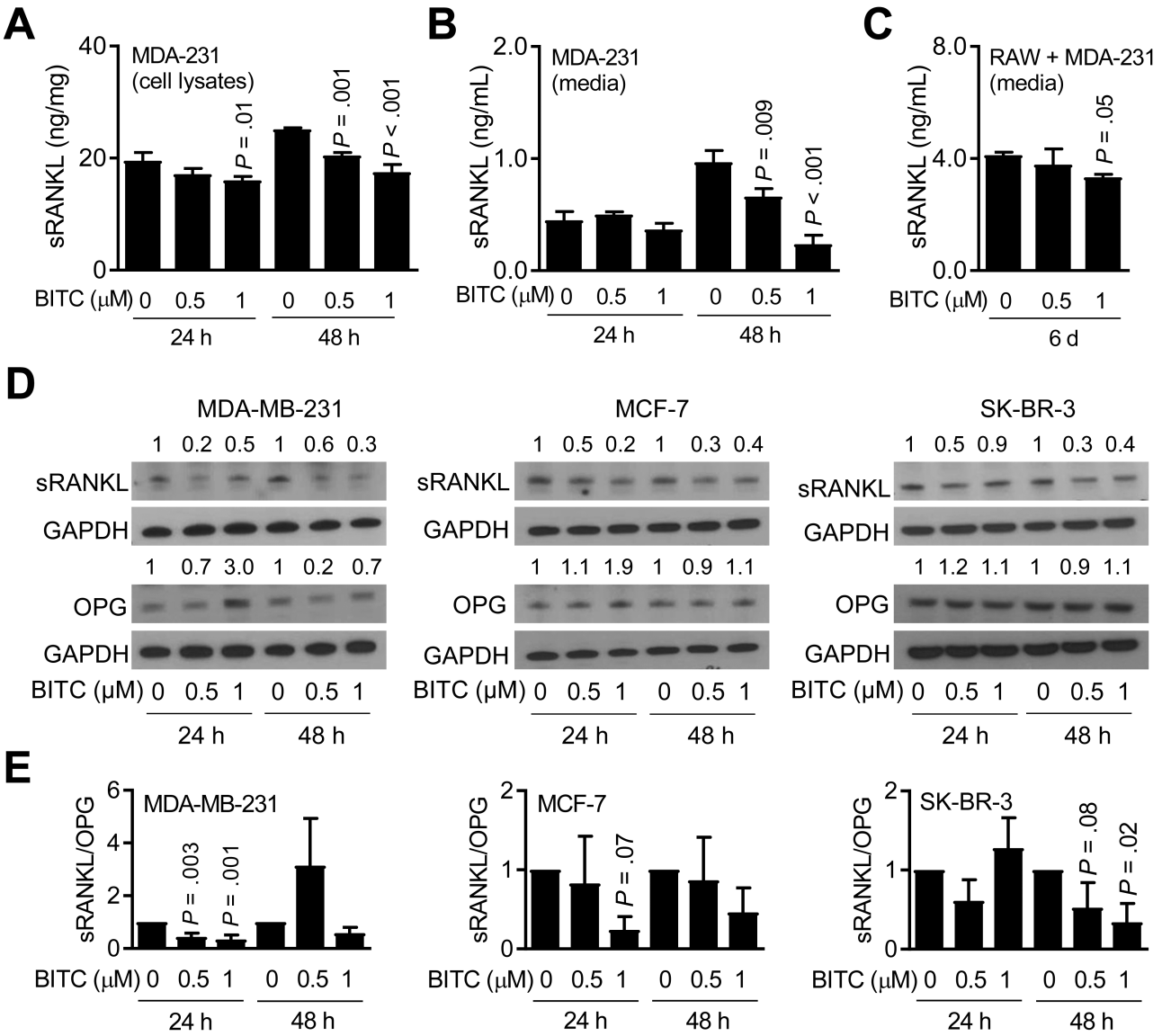

Figure 2. BITC treatment decreases sRANKL expression and secretion. (**A**) Quantitation of intracellular sRANKL level in MDA-MB-231 (MDA-231) cells after 24- or 48-h treatment with DMSO or the indicated doses of BITC. (**B**) Quantitation of sRANKL secretion in CM of MDA-MB-231 (MDA-231) cells after 24- or 48-h treatment with DMSO or the indicated doses of BITC. (**C**) Quantitation of sRANKL secretion in CM of RAW264.7 (RAW) and MDA-MB-231 (MDA-231) co-culture after 6 days of treatment with DMSO or the indicated doses of BITC. For panels (**A–C**), columns indicate average of triplicate samples from a representative experiment, and bars indicate standard deviation. *P* value relative to respective DMSO-treated control was determined by one-way analysis of variance (ANOVA) with Dunnett's adjustment. (**D**) Western blotting for sRANKL, OPG and GAPDH proteins using whole cell lysates from MDA-MB-231, MCF-7 and SK-BR-3 cells after 24- or 48-h treatment with DMSO or the indicated doses of BITC. The numbers above bands represent fold changes of proteins relative to corresponding DMSO-treated control. (**E**) Ratios of quantitative values of sRANKL/OPG from western blotting. Columns indicate average of three different experiments, and bars indicate standard deviation. *P* value relative to respective DMSO-treated control was determined by one-way ANOVA with Dunnett's adjustment. Each experiment was repeated at least three times and the results were consistent.

Kinetics of the skeletal metastasis to the forelimb, hind limb, skull and spine of each mouse of the control and BITC treatment groups is summarized in Supplementary Table 1, available at *Carcinogenesis* Online.

Oral administration of BITC inhibited skeletal metastasis multiplicity by ~81% when compared with control ($P = 0.04$ by unpaired Student's *t*-test) (Figure 5D). Hematoxylin and eosin staining in bone tumor section of mouse # B21L (control) confirmed bone resorption in the area circled in red in Figure 5A of this mouse (Figure 5E). Body weight of mice was not affected by BITC administration (data not shown). These results provided *in vivo* evidence for BITC-mediated inhibition of osteolytic bone resorption.

Effect of BITC on plasma levels of cytokines (bone metastasis study)

Plasma from control- and BITC-treated mice from the experiment described in Figure 5 were used to determine the *in vivo* effect of BITC on levels of cytokines important in skeletal metastasis. RANKL level was lower by ~50% in the plasma of BITC-treated mice when compared with control but the difference was not statistically significant (Supplementary Figure 1a, available at *Carcinogenesis* Online). Cathepsin K activity in the plasma was not affected by BITC administration (Supplementary Figure 1b, available at *Carcinogenesis* Online). However, IL-8 level in the

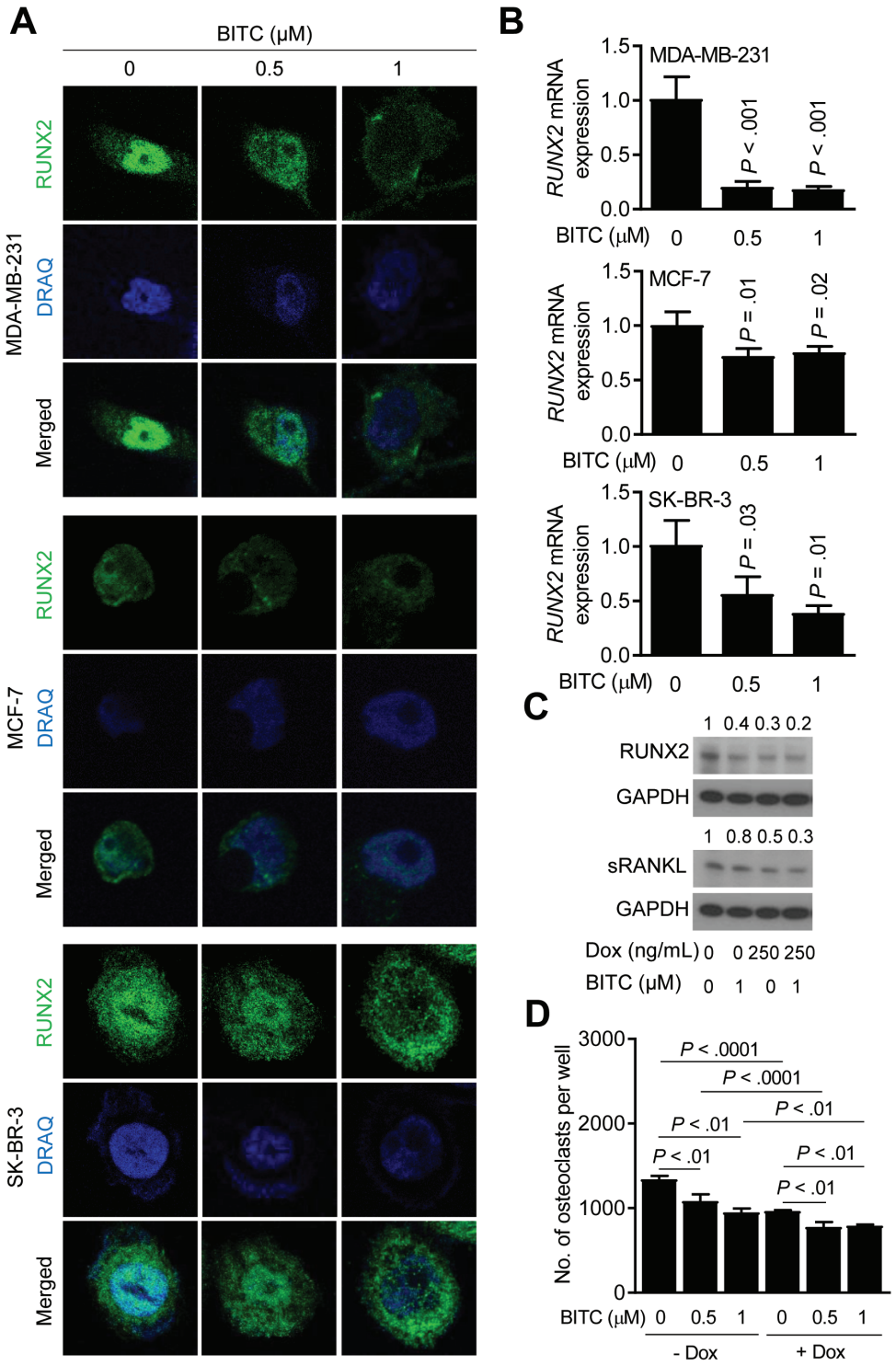

Figure 3. BITC treatment decreases RUNX2 expression in human breast cancer cells. (**A**) Representative confocal images (×63 objective magnification in oil) depicting levels of RUNX2 (green) in MDA-MB-231, MCF-7 and SK-BR-3 cells after 24-h treatment with DMSO or the indicated doses of BITC. Nuclei were stained with DRAQ5 (blue). (**B**) Quantitative real-time polymerase chain reaction analysis for *RUNX2* mRNA expression in MDA-MB-231, MCF-7, and SK-BR-3 cells after 24 h of treatment with DMSO or the indicated doses of BITC. Columns indicate average of triplicate samples of a representative experiment, and bars indicate standard deviation. *P* value was determined by one-way analysis of variance (ANOVA) with Dunnett's adjustment. (**C**) Western blotting for RUNX2 and sRANKL proteins using whole cell lysates of T47D/shRUNX2^{Dox} cells after 24-h treatment with Dox and/or BITC. The numbers above bands represent fold changes of proteins relative to DMSO-treated control. (**D**) Quantitation of osteoclasts from co-culture of RAW264.7 (RAW) and T47D / shRUNX2^{Dox} after 6 days of treatment with DMSO or the indicated doses of BITC. Columns indicate average of triplicate samples of a representative experiment, and bars indicate standard deviation. *P* value was determined by one-way ANOVA followed by Bonferroni's multiple comparison test. Consistent results were obtained from at least two independent experiments.

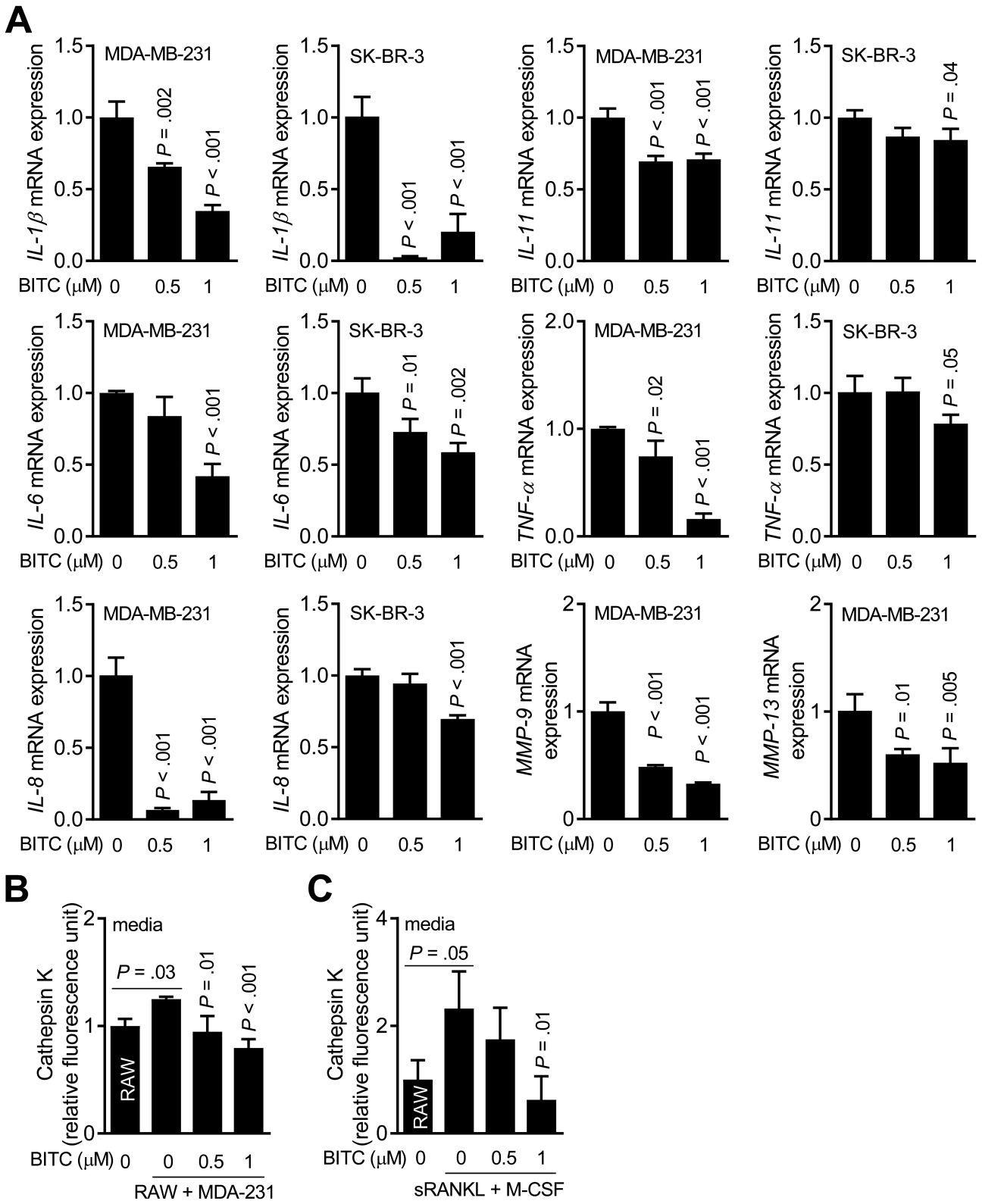

Figure 4. BITC treatment decreases expression of osteoclast regulating factors in human breast cancer cells. (**A**) Quantitative real-time polymerase chain reaction for *IL-1β*, *IL-6*, *IL-8*, *IL-11*, *TNF-α*, *MMP-9* and *MMP-13* mRNA expression in MDA-MB-231 and/or SK-BR-3 cells after 24-h treatment with DMSO or the indicated doses of BITC. Columns indicate average of triplicate samples of a representative experiment, and bars indicate standard deviation. *P* value was determined by one-way analysis of variance (ANOVA) with Dunnett's adjustment. (**B**) Quantitation of Cathepsin K activity in CM of RAW264.7 (RAW) cells alone and RAW + MDA-MB-231 (MDA-231) co-cultures after 6 days of treatment with DMSO or the indicated doses of BITC. Columns indicate average of triplicate samples of a representative experiment, and bars indicate standard deviation. *P* value relative to DMSO-treated co-culture was determined by one-way ANOVA followed by Bonferroni's multiple comparison test. (**C**) Quantitation of Cathepsin K activity in CM of RAW264.7 (RAW) treated for 6 days with sRANKL and M-CSF with or without BITC treatment. Columns indicate average of triplicate samples of a representative experiment, and bars indicate standard deviation. *P* value was determined by one-way ANOVA followed by Bonferroni's multiple comparison test. Consistent results were obtained from at least two independent experiments.

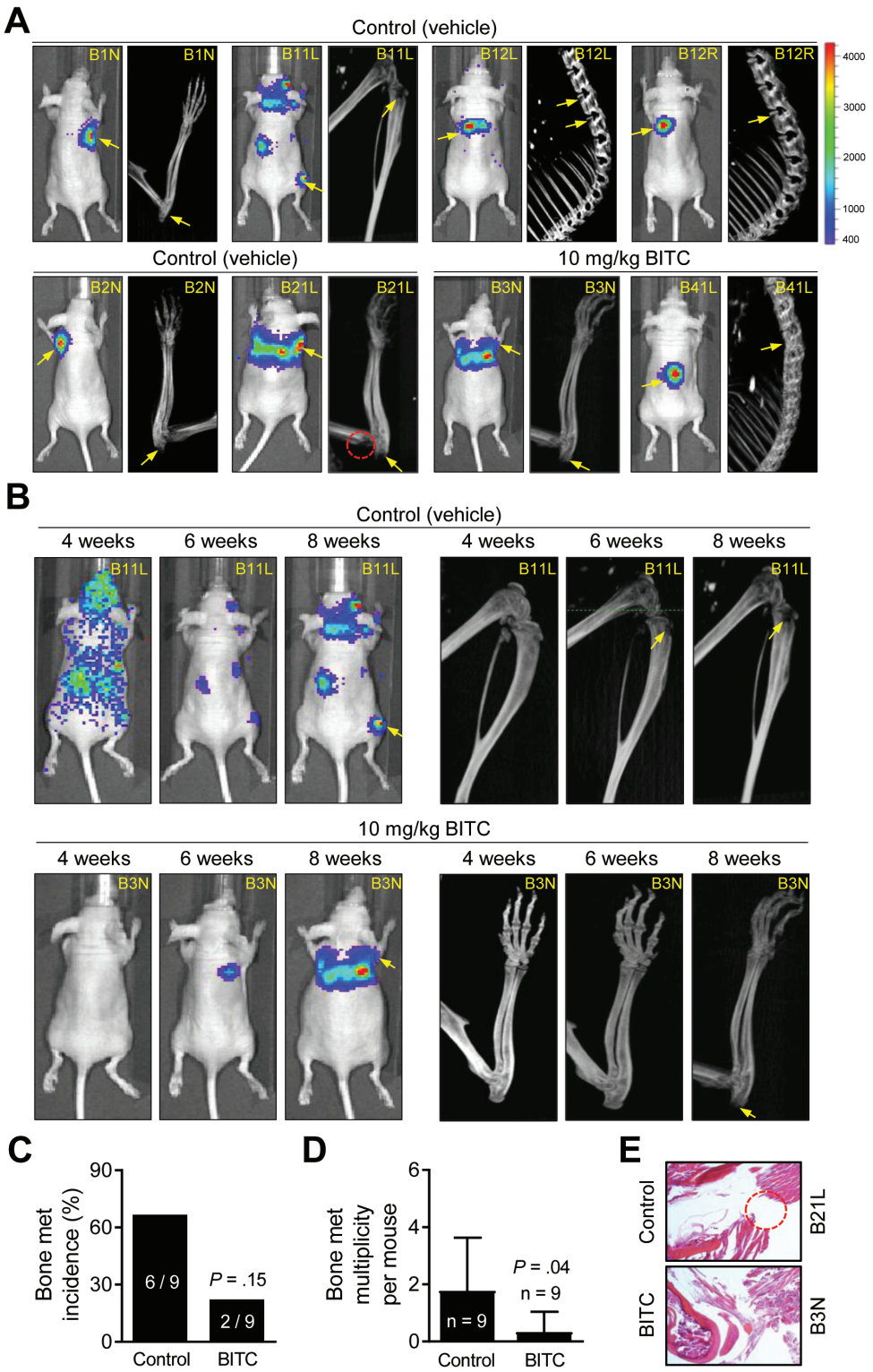

Figure 5. BITC administration inhibits multiplicity of skeletal metastasis induced by intra-cardiac injection of luciferase expressing MDA-MB-231 cells in female nude mice. (**A**) Bioluminescence and bone CT images of control- and BITC-treated mice 8 weeks after cell injection. Bar at right indicates intensity of bioluminescence signal (red is highest and blue is lowest). Yellow arrows and red dotted circle exemplify bone metastasis and osteolytic bone erosion, respectively. (**B**) Longitudinal bioluminescence (left panel) and CT (right panel) imaging of a control mouse (mouse # B11L) and a BITC-treated mouse (mouse # B3N) after intra-cardiac injection of cells. (**C**) Incidence of bone metastases in control- and BITC-treated mice as determined by bioluminescence and CT. *P* value was determined by Fisher's exact test ($n = 9$ for both groups). (**D**) Multiplicity of bone metastasis per mouse in control- and BITC-treated mice at the end of study. Columns indicate average, and bars indicate standard deviation. *P* value was determined by unpaired *t*-test ($n = 9$ for both groups). (**E**) Representative hematoxylin and eosin-stained bone section (×200 magnification) from a control mouse (mouse # B21L) and a BITC-treated mouse (mouse # B3N). Dotted circle indicates bone erosion in mouse # B21L.

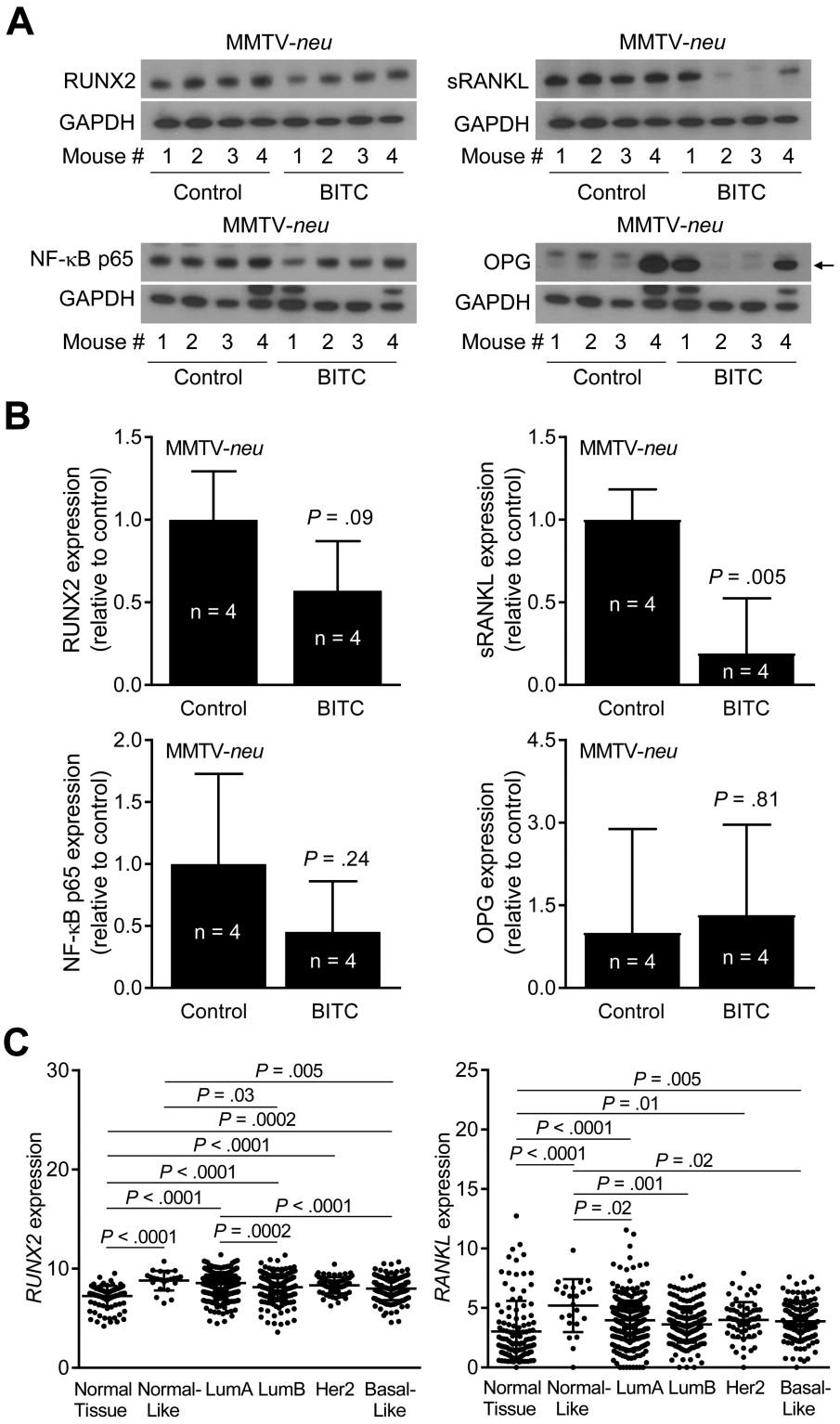

Figure 6. Effect of BITC administration on levels of osteoclast regulating factors in tumors of MMTV-*neu* mice. (**A**) Western blotting for RUNX2, sRANKL, nuclear factor-κB (NF-κB) p65, OPG and GAPDH using MMTV-*neu* tumor supernatants. Arrow indicates right band for OPG protein. (**B**) Quantitation of RUNX2, sRANKL, NF-κB p65 and OPG protein expression in tumors of control- and BITC-treated MMTV-*neu* mice. Columns indicate average and bars indicate standard deviation. *P* value was determined by unpaired Student's *t*-test. (**C**) RNA-seq expression of *RUNX2* and *RANKL* (TCGA dataset) in normal breast tissue ($n = 114$) and breast cancers of different subtypes, including normal-like ($n = 23$), Luminal A (LumA; $n = 421$), LumB ($n = 192$), human epidermal growth factor receptor 2 ($n = 67$) and basal-like ($n = 141$). *P* value was determined by one-way ANOVA with Bonferroni's test.

plasma of BITC-treated mice was lower by ~90% when compared with that of control mice (Supplementary Figure 1c, available at *Carcinogenesis* Online; $P = 0.007$ by unpaired Student's *t*-test).

Luminex-based cytokine profiling also revealed a statistically significant decrease in plasma IL-1β level in the BITC treatment group compared with control ($P = 0.03$ by two-sided unpaired Student's *t*-test) (Supplementary Figure 1d, available at *Carcinogenesis* Online). These results indicated BITC-mediated decrease in circulating levels of a few cytokines important for tumor growth and bone metastasis.

Effect of BITC treatment on mammary tumor levels of RUNX2, sRANKL and OPG (MMTV-*neu* study)

We have shown previously that dietary administration of BITC to MMTV-*neu* transgenic mice results in reduction of breast cancer incidence (23). Figure 6A shows western blots for RUNX2, sRANKL, nuclear factor-κB p65 and OPG expression in mammary tumors of MMTV-*neu* mice. Similar to the results from cultured breast cancer cells, protein level of sRANKL was significantly lower in tumors of BITC-treated MMTV-*neu* mice when compared with control ($P = 0.005$ by two-sided unpaired Student's *t*-test) (Figure 6B).

RUNX2 and *RANKL* expression in different subtypes of breast cancer

Next, we compared *RUNX2* and *RANKL* RNA-seq expressions (TCGA dataset) in normal breast tissue ($n = 114$) and breast cancers of different subtypes, including normal-like ($n = 23$), Luminal A (LumA; $n = 421$), Luminal B (LumB; $n = 192$), human epidermal growth factor receptor 2 ($n = 67$) and basal-like ($n = 141$). Expression of both *RUNX2* and *RANKL* was significantly higher in most subtypes of breast cancer when compared with normal breast tissue (Figure 6C).

Discussion

The current standard of care for patients with bone metastasis for reducing the incidence of skeletal complications includes bisphosphonates (e.g. clodronate, zoledronate, etc.) and anti-RANKL antibody denosumab (12,13,44,45). However, a subset of patients on these therapies still develops new bone metastasis or experience adverse effects (12,13,44,45). Bisphosphonates have poor oral bioavailability. Therefore, orally bioavailable and non-toxic inhibitors of breast cancer-induced osteoclast differentiation are still clinically attractive. The present study provides *in vivo* evidence for BITC-mediated inhibition of breast cancer-induced osteolytic bone resorption. Of note, complete regression of skeletal metastasis was observed in some mice of BITC treatment group (Supplementary Table 1, available at *Carcinogenesis* Online).

It is important to mention that MDA-MB-231 is the best-characterized and most reliable cellular model for the *in vivo* study of human breast cancer-induced osteolytic bone resorption (46–50). Intra-cardiac injection of MDA-MB-231 cells in immune compromised mice reproducibly results in osteolytic bone lesions (45,47). Other commonly used breast cancer cell lines such as MCF-7 or SK-BR-3 either poorly colonize to the bone or tend to form mixed osteoblastic or osteosceleretic lesions unlike osteolytic bone erosion prevalent in women with metastatic breast cancer (46–50). Bone resorption or skeletal metastasis is not observed in chemically-induced or transgenic models of breast cancer. Further studies are needed to determine whether osteolytic bone resorption induced by cell lines other than MDA-MB-231 is inhibited by BITC treatment.

The osteoclast activity is stimulated by several cytokines produced by the breast tumor cells, including IL-8, IL-1 and IL-6 (6–10). This study reveals that the BITC-mediated inhibition of osteolytic differentiation *in vitro* and bone resorption *in vivo* is associated with suppression of mRNA or protein expression (breast cancer cells) and/or secretion (CM or plasma of mice) of IL-1β, IL-6 and/or IL-8. It is reasonable to propose that these changes probably contribute to BITC-mediated inhibition of osteolytic bone resorption.

RANKL is one of the most important molecules in regulation of osteoclast activation, function and survival (34–36). Normal bone remodeling involves interaction of RANKL expressed on osteoblasts with RANK on osteoclast precursors to stimulate their differentiation. However, RANKL is also expressed in breast tumors of different subtypes as revealed by our own analysis of RNA-seq data from TCGA. The present study reveals a critical role for RUNX2-sRANKL axis in BITC-mediated inhibition of osteolytic bone resorption based on following observations: (i) BITC decreases sRANKL protein expression and secretion in breast cancer cells; (ii) prevention of osteolytic bone resorption by BITC *in vivo* is accompanied by suppression of plasma RANKL level; (iii) chemoprevention of breast cancer by BITC in MMTV-*neu* mice is also associated with sRANKL protein downregulation in the mammary tumor; (iv) BITC treatment suppresses mRNA and protein levels of RUNX2, which regulates RANKL expression (35,38,39) and (v) RUNX2 knockdown in breast cancer cells augments BITC-mediated downregulation of sRANKL and suppression of breast cancer cell-induced osteoclast differentiation.

In conclusion, the present study shows prevention of breast cancer-induced osteolytic bone resorption by oral administration of BITC. Mechanistic studies point to a critical role for RUNX2–RANKL axis in BITC-mediated inhibition of breast cancer cell-induced osteoclast differentiation and osteolytic bone erosion.

Supplementary material

Supplementary data are available at *Carcinogenesis* online.

Funding

National Cancer Institute (NCI), National Institutes of Health, USA [RO1 CA129347 and P30 CA047904].

Acknowledgments

This research project used the Animal Facility, the Biostatistics Facility, the *In Vivo* Imaging Facility, the Proteomics Facility (Luminex) and the Tissue and Research Pathology Facility supported, in part, by a grant from the NCI (P30 CA047904; Principal Investigator—Dr Robert L. Ferris).
Conflict of Interest Statement: None declared.

References

1. Kelsey, J.L. *et al.* (1993) Reproductive factors and breast cancer. Epidemiol. Rev., 15, 36–47.
2. Hulka, B.S. *et al.* (1995) Breast cancer: cause and prevention. Lancet, 346, 883–887.
3. van Zitteren, M. *et al.* (2011) Genome-based prediction of breast cancer risk in the general population: a modeling study based on meta-analyses of genetic associations. Cancer Epidemiol. Biomarkers Prev., 20, 9–22.
4. Perou, C.M. *et al.* (2000) Molecular portraits of human breast tumours. Nature, 406, 747–752.
5. Siegel, R.L. *et al.* (2016) Cancer statistics, 2016. CA. Cancer J. Clin., 66, 7–30.

6. Weigelt, B. *et al.* (2005) Breast cancer metastasis: markers and models. Nat. Rev. Cancer, 5, 591–602.
7. Coleman, R.E. (2002) Future directions in the treatment and prevention of bone metastases. Am. J. Clin. Oncol., 25 (6 Suppl. 1), S32–S38.
8. Mundy, G.R. (2002) Metastasis to bone: causes, consequences and therapeutic opportunities. Nat. Rev. Cancer, 2, 584–593.
9. Weilbaecher, K.N. *et al.* (2011) Cancer to bone: a fatal attraction. Nat. Rev. Cancer, 11, 411–425.
10. Le Pape, F. *et al.* (2016) The role of osteoclasts in breast cancer bone metastasis. J. Bone Oncol., 5, 93–95.
11. Kennecke, H. *et al.* (2010) Metastatic behavior of breast cancer subtypes. J. Clin. Oncol., 28, 3271–3277.
12. Kennel, K.A. *et al.* (2009) Adverse effects of bisphosphonates: implications for osteoporosis management. Mayo Clin. Proc., 84, 632–7; quiz 638.
13. Manzaneque, A. *et al.* (2017) Use and safety of denosumab in cancer patients. Int. J. Clin. Pharm., 39, 522–526.
14. Lee, K.W. *et al.* (2011) Molecular targets of phytochemicals for cancer prevention. Nat. Rev. Cancer, 11, 211–218.
15. Rao, C.V. *et al.* (2012) Mitosis-targeting natural products for cancer prevention and therapy. Curr. Drug Targets, 13, 1820–1830.
16. Hao, F. *et al.* (2014) Neem components as potential agents for cancer prevention and treatment. Biochim. Biophys. Acta, 1846, 247–257.
17. Lu, J. *et al.* (2007) Oriental herbs as a source of novel anti-androgen and prostate cancer chemopreventive agents. Acta Pharmacol. Sin., 28, 1365–1372.
18. Ambrosone, C.B. *et al.* (2004) Breast cancer risk in premenopausal women is inversely associated with consumption of broccoli, a source of isothiocyanates, but is not modified by GST genotype. J. Nutr., 134, 1134–1138.
19. Liu, X. *et al.* (2013) Cruciferous vegetables intake is inversely associated with risk of breast cancer: a meta-analysis. Breast, 22, 309–313.
20. Singh, S.V. *et al.* (2012) Cancer chemoprevention with dietary isothiocyanates mature for clinical translational research. Carcinogenesis, 33, 1833–1842.
21. Thomson, C.A. *et al.* (2016) Chemopreventive properties of 3,3'-diindolylmethane in breast cancer: evidence from experimental and human studies. Nutr. Rev., 74, 432–443.
22. Wattenberg, L.W. (1977) Inhibition of carcinogenic effects of polycyclic hydrocarbons by benzyl isothiocyanate and related compounds. J. Natl. Cancer Inst., 58, 395–398.
23. Warin, R. *et al.* (2009) Prevention of mammary carcinogenesis in MMTV-neu mice by cruciferous vegetable constituent benzyl isothiocyanate. Cancer Res., 69, 9473–9480.
24. Tomaskovic-Crook, E. *et al.* (2009) Epithelial to mesenchymal transition and breast cancer. Breast Cancer Res., 11, 213.
25. Creighton, C.J. *et al.* (2010) Epithelial-mesenchymal transition (EMT) in tumor-initiating cells and its clinical implications in breast cancer. J. Mammary Gland Biol. Neoplasia, 15, 253–260.
26. Sehrawat, A. *et al.* (2011) Benzyl isothiocyanate inhibits epithelial-mesenchymal transition in cultured and xenografted human breast cancer cells. Cancer Prev. Res. (Phila)., 4, 1107–1117.
27. Xiao, D. *et al.* (2003) Allyl isothiocyanate, a constituent of cruciferous vegetables, inhibits proliferation of human prostate cancer cells by causing G2/M arrest and inducing apoptosis. Carcinogenesis, 24, 891–897.
28. Hahm, E.R. *et al.* (2013) Metabolic alterations in mammary cancer prevention by withaferin A in a clinically relevant mouse model. J. Natl. Cancer Inst., 105, 1111–1122.
29. Powolny, A.A. *et al.* (2011) Chemopreventative potential of the cruciferous vegetable constituent phenethyl isothiocyanate in a mouse model of prostate cancer. J. Natl. Cancer Inst., 103, 571–584.
30. Livak, K.J. *et al.* (2001) Analysis of relative gene expression data using real-time quantitative PCR and the 2(-Delta Delta C(T)) method. Methods, 25, 402–408.
31. Fang, Y. *et al.* (2013) Inhibition of breast cancer metastases by a novel inhibitor of TGFβ receptor 1. J. Natl. Cancer Inst., 105, 47–58.
32. Boreddy, S.R. *et al.* (2011) Pancreatic tumor suppression by benzyl isothiocyanate is associated with inhibition of PI3K/AKT/FOXO pathway. Clin. Cancer Res., 17, 1784–1795.
33. Subik, K. *et al.* (2010) The expression patterns of ER, PR, HER2, CK5/6, EGFR, Ki-67 and AR by immunohistochemical analysis in breast cancer cell lines. Breast Cancer (Auckl)., 4, 35–41.
34. Dougall, W.C. (2012) Molecular pathways: osteoclast-dependent and osteoclast-independent roles of the RANKL/RANK/OPG pathway in tumorigenesis and metastasis. Clin. Cancer Res., 18, 326–335.
35. Yoneda, T. *et al.* (2013) Role of RANKL/RANK in primary and secondary breast cancer. World J. Orthop., 4, 178–185.
36. González-Suárez, E. *et al.* (2016) RANK as a therapeutic target in cancer. FEBS J., 283, 2018–2033.
37. Enomoto, H. *et al.* (2003) Induction of osteoclast differentiation by Runx2 through receptor activator of nuclear factor-kappa B ligand (RANKL) and osteoprotegerin regulation and partial rescue of osteoclastogenesis in Runx2-/- mice by RANKL transgene. J. Biol. Chem., 278, 23971–23977.
38. Pratap, J. *et al.* (2006) Regulatory roles of Runx2 in metastatic tumor and cancer cell interactions with bone. Cancer Metastasis Rev., 25, 589–600.
39. Wysokinski, D. *et al.* (2015) Role of RUNX2 in breast carcinogenesis. Int. J. Mol. Sci., 16, 20969–20993.
40. Roodman, G.D. (2004) Mechanisms of bone metastasis. N. Engl. J. Med., 350, 1655–1664.
41. Guise, T.A. *et al.* (2006) Basic mechanisms responsible for osteolytic and osteoblastic bone metastases. Clin. Cancer Res., 12(20 Pt 2), 6213s–6216s.
42. Le Gall, C. *et al.* (2008) Cathepsin K inhibitors as treatment of bone metastasis. Curr. Opin. Support. Palliat. Care, 2, 218–222.
43. Le Gall, C. *et al.* (2007) A cathepsin K inhibitor reduces breast cancer induced osteolysis and skeletal tumor burden. Cancer Res., 67, 9894–9902.
44. Stresing, V. *et al.* (2007) Bisphosphonates in cancer therapy. Cancer Lett., 257, 16–35.
45. Gnant, M. *et al.*; Austrian Breast and Colorectal Cancer Study Group. (2015) Adjuvant denosumab in breast cancer (ABCSG-18): a multicentre, randomised, double-blind, placebo-controlled trial. Lancet, 386, 433–443.
46. Hibberd, C. *et al.* (2013) Animal cancer models of skeletal metastasis. Cancer Growth Metastasis, 6, 23–34.
47. Simmons, J.K. *et al.* (2015) Animal Models of Bone Metastasis. Vet. Pathol., 52, 827–841.
48. Duivenvoorden, W.C. *et al.* (2007) Effect of zoledronic acid on the doxycycline-induced decrease in tumour burden in a bone metastasis model of human breast cancer. Br. J. Cancer, 96, 1526–1531.
49. Hergueta-Redondo, M. *et al.* (2014) Gasdermin-B promotes invasion and metastasis in breast cancer cells. PLoS One, 9, e90099.
50. Tarragona, M. *et al.* (2012) Identification of NOG as a specific breast cancer bone metastasis-supporting gene. J. Biol. Chem., 287, 21346–21355.